Influence of stress and defects on the silicon-terminated SiC(001) surface structure

Alessandra Catellani
CNR-MASPEC, Via Chiavari, 18/A, I-43100 Parma, Italy

Giulia Galli and François Gygi
Institut Romand de Recherche Numérique en Physique des Matériaux (IRRMA), CH-1015 Lausanne, Switzerland

Fabio Pellacini
CNR-MASPEC, Via Chiavari, 18/A, I-43100 Parma, Italy
and Department of Physics, University of Parma, Viale delle Scienze, I-43100 Parma, Italy
(Received 26 November 1997; revised manuscript received 23 January 1998)

Using *ab initio* calculations, we have investigated the influence of stress and defects on the reconstruction of the (001) Si-terminated surface of cubic SiC. We find that an unstrained bulk is terminated by a $p(2\times1)$ reconstruction under tensile stress. This stress can be substantially relieved by the removal of dimers. Applying further tensile stress lowers the surface symmetry and leads to a $c(4\times2)$ pattern. The structural properties of this reconstruction are in very good agreement with recent measurements, suggesting that stress in SiC samples is responsible for the $c(4\times2)$ reconstruction observed experimentally. Furthermore, we have analyzed temperature and charging effects on the surface properties and made a comparative study of theoretical and experimental STM images. [S0163-1829(98)07019-2]

I. INTRODUCTION

Nowadays many properties of the surface reconstructions of elemental semiconductors are well understood, whereas the characterization of compound surfaces is much less advanced, due to the complexity of covalent bonds involving multiple species. Among compound semiconductors, the surface properties of SiC have been the subject of intense research.[1] A thorough characterization of SiC surfaces is an essential prerequisite to understanding the growth of the material, as well as its applications as a semiconductor for high-power, high-temperature, and high-radiation environments.[2]

The most studied[1] face of the cubic polytype of SiC (β-SiC) is the (001), the (111) surface being essentially identical to the (0001) surface of the hexagonal phase. Although recent investigations[3–5] have shed some light on SiC(001) surfaces, many properties of the Si-terminated face are still the subject of debate.[1] Experimentally both $p(2\times1)$ (Refs. 6 and 7) and $c(4\times2)$ (Ref. 7) LEED patterns have been reported on clean Si-terminated surfaces. Furthermore, recent STM data[8,9] have revealed a $c(4\times2)$ geometry and a $p(2\times1)$ pattern in areas of missing dimers. A structural analysis[6] of the $p(2\times1)$ pattern has led to a buckled-dimer model similar to that of Si(001), with very short dimers (2.31 Å). However, this model is not confirmed by *ab initio* calculations,[4,5] reporting instead unbuckled dimers much longer than those of Si(001); moreover, very recent ARUPS data[10] are consistent with a weak bonding of the Si dimers.

Cubic SiC films are presently prepared by chemical vapor deposition on Si(001) substrates. Since the lattice mismatch between Si and SiC is almost 20%, SiC samples grown on Si are expected to be strained. This is indicated, e.g., by LEED spots that are not as sharp as those of well ordered bulk single-crystal surfaces,[1] and by anomalously broad Si $2p$ levels obtained in core-level spectroscopy.[7,11] While the influence of stress on surface reconstruction has been recognized for several elemental semiconductors,[12] no investigation of stress effects on cubic SiC surfaces has been reported to date.

In this paper we present a study of the influence of stress and defects on the reconstruction of the Si-terminated β-SiC(001) surface. Using *ab initio* calculations,[13,14] we analyzed the effect of both tensile and compressive stresses and that of missing dimers on the surface. Our results allow us to rationalize several measurements,[6,7] and in particular to interpret very recent STM data.[8,9] Furthermore, we give predictions about surface energy, surface stress, and tension: these are crucial quantities both in growth processes and in interface formation, and their experimental determination still remains a difficult task. Finally, we discuss the effect of temperature and extra charges on the surface structure.

The rest of the paper is organized as follows. In Sec. II we describe our computational approach. In Secs. III and IV we discuss the results of our calculations at zero temperature, for a Si-terminated surface of an unstrained and strained bulk, respectively. In Sec. V we discuss some finite temperature properties of Si-terminated surfaces, and in Sec. VI we compare calculated STM images to the available experimental data. Finally, Sec. VII concludes the paper.

II. COMPUTATIONAL APPROACH

Our calculations were carried out within the local density functional approximation. We used slabs periodically repeated in the (x,y) plane, terminated on each side by a layer containing Si atoms, followed by a vacuum region of $\simeq$8.5 Å. We carried out one series of computations with supercells containing eight-atom layers, with a number of layers varying from 11 to 19. A second series of computations was performed with supercells containing 16- and 32-atom lay-

ers, with 11 and 6 layers, respectively. The interaction between ionic cores and valence electrons was described by nonlocal pseudopotentials.[15] In deriving these pseudopotentials, we used cutoff radii $r_c = 0.85$ and 0.80 a.u. for the s and p wave functions of C (s-only nonlocality), and $r_c = 1.05$, 1.28, and 1.28 for the s, p, and d wave functions of Si (s and p nonlocality). We considered Bloch functions at the Γ point of the supercell surface Brillouin zone (SBZ), which were expanded in plane waves with a kinetic energy cutoff ($E_{\rm cut}$) of 40 Ry (160 Ry for the charge density). Using 8, 16, and 32 atoms per layer corresponds to including 3, 6, and 8 points in the irreducible wedge of the $p(2\times1)$ SBZ, respectively.

In our computations we evaluated total energies and equilibrium geometries, as well as surface energies, stresses, and tensions. The surface energy was defined as $e_s = \lim_{N_l\to\infty}[E_{\rm slab} - N_l E_{\rm bulk}]$, where $E_{\rm slab}$ and N_l are, respectively, the cohesive energy and number of layers in the slab; $E_{\rm bulk}$ is the cohesive energy of the bulk computed as the slope of the function $E_{\rm slab}(N_l)$.[16] We extrapolated $E_{\rm bulk}$ and then e_s from three calculations with $N_l = 11$, 15, and 19, using supercells with 8 atoms per layer.

Furthermore, we computed the stress parallel and perpendicular to the surface dimers. In a slab of edges a_0, b_0, c_0 for $a_0 = b_0 = a_{\rm eq}$, with the dimer row along one cell edge (a), the stresses parallel and perpendicular to the dimers are $\sigma_\parallel = b_0(\partial E/\partial a)|_{a_0}$ and $\sigma_\perp = a_0(\partial E/\partial b)|_{b_0}$, respectively. The surface tension at zero temperature is given by $\gamma = (1/2a_0^2)\mathrm{Tr}[\sigma]$. We computed $(\partial E/\partial a)|_{a_0}$ and σ using different cutoffs ($E_{\rm cut} = 40$ and 58 Ry). Moreover, we varied the size of the supercell by considering slabs containing 8 and 16 atoms per layer and 11 layers, and slabs with 11 and 19 layers and 8 atoms per layer. This allowed us to estimate an error of ± 0.25 eV/atom on the value of γ.

III. Si-TERMINATED SURFACE OF AN UNSTRAINED BULK

Using the approach outlined above, we first studied the reconstruction of the clean surface of an unstrained bulk, and then analyzed the influence of defects, and in particular of a missing dimer, on the structural and electronic properties of this surface. We used slabs with the periodicity of the unstrained bulk and performed our calculations at the equilibrium theoretical lattice constant[5] of bulk SiC ($a_{\rm eq} = 4.30$ Å).

A. Structural and elastic properties of the clean surface

Given the apparent disagreement on the reconstruction of Si-SiC(001) between *ab initio* calculations[4,5] and LEED measurements,[6] we performed an extensive sampling of the potential energy surface of β-SiC(001) [Si-SiC(001)], in order to determine the most stable reconstruction. We note that the Si-terminated ideal surface of Si-SiC(001) is a metastable, nonmetallic configuration with a gap between occupied π^*-like and empty σ-like surface states.[4,5] This differs from the (001) ideal surfaces of Si, C,[17,18] and C-SiC(001),[4,5] which are metallic unstable surfaces. In our calculations, we find that the ideal Si-SiC(001) surface is under tensile stress (2.1 eV/atom).

The potential energy of Si-SiC(001) is extremely flat as surface atoms move in the plane parallel to the surface,[4,5] and particular care must be taken in the sampling procedure, when looking for the most stable reconstruction. We carried out total energy global optimizations using molecular dynamics and starting from a series of different initial configurations. These include several $c(4\times2)$ geometries, with dimers having different lengths (in the interval 2.2–2.8 Å) and buckling. We considered both the $c(4\times2)$ geometry of the Si(001) reconstructed surface[17] and the $c(4\times2)$ geometry proposed in Refs. 8 and 9. We also devised starting configurations with symmetries lower than $c(4\times2)$. All of these configurations turned out to be unstable. Irrespective of the starting point of our calculations, we found the same stable minimum at the end of each optimization procedure. The most stable reconstruction is a weak $p(2\times1)$ pattern with unbuckled dimer rows, having a total energy a few meV/atom lower than that of the ideal surface. We note that the surface symmetry is independent of the lateral supercell size, i.e., of the k-point sampling of the SBZ; on the contrary, the dimer bond length varies from 2.58 to 2.63 Å, when going from 8-atom to 16-atom layers. These distances are much larger than the value deduced from fits of LEED patterns by Powers *et al.*[6] (2.31 Å). These authors assumed a buckled dimer geometry, which might lead to errors in the resulting distances. Furthermore, temperature,[5] stress, and charging effects could be responsible for reconstructions different from those observed at equilibrium (see below).

In order to fully characterize the $p(2\times1)$ reconstruction of Si-SiC(001), we computed the surface energy (e_s), stress (σ_{ii}), and tension (γ). The value of e_s is 2.7 eV/atom, close to the formation energy of a Si-C bond, indicating the quasi-ideal character of the surface. This energy is much higher than the surface energies of the three reconstructions of C-SiC(001), which vary between 1.5 and 1.7 eV/atom.

In our calculations[19] we find that the $p(2\times1)$ reconstruction of Si-SiC(001) lowers the tensile stress present in the ideal geometry to $\simeq$ 1.1 eV/atom and $\simeq$ 1.9 eV/atom in the directions parallel and perpendicular to the dimers, respectively. This is at variance with the corresponding reconstruction of Si(001), where the stress is tensile in the direction of the dimers (1.6 eV/atom) and compressive (-0.9 eV/atom) in the perpendicular direction.[20] We note that the surface tension of Si-SiC(001) (1.7 ± 0.2 eV/atom, i.e., 2956 ± 346 erg/cm^2) is very close to that of the corresponding $p(2\times1)$ carbon-terminated surface (2970 erg/cm^2), but differs substantially from those of the $c(2\times2)$ faces of C-SiC(001) (5365 and 575 erg/cm^2 for the staggered dimer and bridge geometries, respectively).

B. Electronic properties of the clean surface

We now turn to the discussion of the electronic properties of the $p(2\times1)$ reconstructed surface. Similar to the ideal configuration, this surface is nonmetallic, with a gap of about 0.3 eV between π^*-like and σ-like surface states. This is again different from the electronic structure of the Si(001) and C(001) surfaces[17,18] where the reconstruction opens a band gap between π and π^* surface states. Another relevant difference between SiC(001) and the corresponding Si and C surfaces concerns the electron affinity. In our calculation we

found that the vacuum level (VL) of Si-SiC(001) is lower in energy than the conduction-band bottom (CBB), i.e., the surface has a negative electron affinity (EA). Similarly we found that the C terminated surfaces of SiC(001) have a negative EA, while Si(001) (Ref. 21) and C(001) (Ref. 18) have a positive EA. The difference EA=CBB−VL has been computed by aligning the averages of the self-consistent potential in the bulk and in the slab.[22] The CBB has been evaluated using the experimental (2.4 eV) instead of the computed (1.28 eV) bulk band gap. The value of EA is very sensitive to the number of layers in the slab, increasing when increasing the number of layers from 11 to 15 and 19. It is much less sensitive to the number of atoms per layer, i.e., to the k-point sampling in the plane of the surface. For a 19 layer slab, with 8 atoms per layer, we obtain that the VL is about 0.9 eV lower than the CBB.

Since the $p(2\times1)$ reconstructed surface has a negative EA, it is interesting to investigate changes in the electronic and structural properties of this system when it loses electrons, i.e., it is positively charged. We have carried out a qualitative investigation of charging effects on the surface by optimizing the surface structure of an unstrained bulk with missing electrons, corresponding to $\simeq\pm0.4$ electrons per surface atom. This has been done by removing 12 electrons from a periodically repeated slab with two surfaces and containing 176 atoms, i.e., 704 electrons. A uniform negative background was added to neutralize the system. The electrons turned out to be missing from surface states. Their removal causes important modifications of the surface structure, in particular a large decrease in the dimer bond length (to about 2.4 Å), accompanied by an increase of some of the Si-C bonds between the first and the second surface layer. A stronger bond between dimers is favored by a depletion of charge in the highest occupied surface state, which has large antibonding components. We have also studied the case of a negatively charged surface, where we observe structural modifications opposite to those found for the positively charged system: the dimer bond length becomes longer than in the neutral surface and some of the Si-C bonds between the first and the second surface layer become considerably shorter. Therefore we conclude that perturbations of the surface leading to a charging of the system may substantially affect its geometry and in particular change the bonding characteristics of the surface dimers.

C. Influence of a missing dimer on the surface

Experimentally $p(2\times1)$ reconstructions of Si-SiC(001) have been often seen in areas of missing dimers[8] and low coverage.[7] It is therefore of interest to study a $p(2\times1)$ reconstructed surface with missing dimers, in order to analyze how these defects influence the reconstruction pattern. We have carried out such a study using a slab with a defect density equal to 1/16. We performed our calculation with 32 atoms per layer and 6 layers, with a missing dimer on the uppermost layer. The slab was Si-terminated on the top and C-terminated, with a semiconducting bridge reconstruction,[5] on the bottom. Only the three uppermost layers were mobile.

We found that the removal of a dimer induces the formation of stronger bonds in four dimers surrounding the missing unit: the bond length of two dimers parallel to the defect becomes 2.37 Å and that of two adjacent buckled dimers in parallel rows is decreased to 2.46 Å. Nevertheless, a dimer removal does not constitute a long-ranged perturbation on the $p(2\times1)$ reconstruction, whose symmetry and dimer bond lengths are basically unchanged. Furthermore, we found that removing a dimer lowers the surface tension considerably (by about 25% in our slab). Therefore, we conclude that missing dimers allow the surface to relieve stress and thus help to stabilize the $p(2\times1)$ reconstruction, in agreement with experimental observations.[7] Removal of dimers could be a mechanism for stress relief also in the presence of a bulk under tensile stress, where the surface tension is expected to increase.

IV. Si-TERMINATED SURFACE OF A BULK UNDER STRESS

In order to investigate if the surface reconstruction is sensitive to the presence of a strained bulk, we performed three series of calculations. First, we considered a slab under uniform tensile stress, by increasing isotropically in x and y the bulk volume (Ω) by $\simeq2\%$ with respect to its equilibrium value ($\Omega_{\rm eq}$). We also applied stresses of opposite signs (variation of $\simeq\pm3\%$ in the lattice constant) in the x and y directions, keeping the volume equal to $\Omega_{\rm eq}$. Finally, we applied a tensile stress in the y direction, keeping the cell length in the x direction equal to its equilibrium value. In this case, we increased the value of the lattice constant along y by 7%, which corresponds to the change observed in recent STM experiments.[8] We also studied the deformation in which the cell length in the y direction is equal to its equilibrium value, and the lattice constant along x is increased by 7%. All of these calculations were carried out with 11 layers, each containing 16 atoms, with dimers oriented along the x direction.

When applying a uniaxial compressive stress along the dimers, the symmetry of the surface is unchanged and the dimer bond length increases (2.75 Å) with respect to that of the unstrained bulk. This indicates that under uniaxial compressive stresses in the direction parallel to the dimers, the surface tends to adopt an ideal geometry. On the contrary, when applying either a uniform tensile stress or a uniaxial tensile stress along the dimers, a change in the surface reconstruction is observed, in particular a symmetry breaking leading to a $c(4\times2)$ reconstruction. A very weak $c(4\times2)$ reconstruction, of the same kind, is obtained also when applying a tensile stress in the y direction, while keeping the lattice constant in the x direction equal to its equilibrium value. This corresponds to the case observed in STM measurements.[8]

When applying a tensile stress to the surface, in all cases considered in our study we obtain a $c(4\times2)$ reconstruction that is characterized by alternating unbuckled short and long dimers, with the short dimers having a smaller z component than the long ones. The dimer bond lengths and the difference in z coordinates between long and short dimers depend on the applied stress. The dimer bond lengths are 2.54 and 2.62 Å in the case of a uniform stress. When applying a uniaxial stress, we find bond distances equal to 2.53 and 2.59 Å, for a 3% increase of the lattice constant in the x direction; in the case of a 7% increase, these distances become $\simeq$ 2.40

and $\simeq 2.55$ Å. The difference in the z coordinate is 0.06 Å for a stress corresponding to a 3% increase of the lattice constant. This value is approximately doubled in the case of a 7% increase. The weak $c(4\times2)$ reconstruction found in the case of a uniaxial stress along y has dimers of length 2.60 and 2.57 Å, with the short dimers having a z component smaller than the long ones by about 0.02 Å. We note that when a $c(4\times2)$ reconstruction takes place, the second surface layer of C atoms participates in the geometrical arrangement by a slight adjustment, in order to keep the Si-C distances equal to their bulk value.

The $c(4\times2)$ reconstruction found in our calculation is substantially different from that of Si(001) and is in very good agreement with the alternating-up-and-down-dimer (AUDD) model recently proposed on the basis of STM experiments.[8,9] However, these experiments do not discriminate between short and long dimers and thus the authors of Refs. 8 and 9 assumed that all dimers have the same bond length. We note that $c(4\times2)$ reconstructions on clean surfaces have also been detected in x-ray photoemission experiments.[7] Our results indicate that samples used experimentally should be under tensile stress, which is conceivable since all of them have been grown on Si(001). As discussed above, stress relief could come from removal of dimers, which should stabilize a $p(2\times1)$ reconstruction. Chemical contamination of $c(4\times2)$ could be another way of relieving stress and thus give rise to $p(2\times1)$ patterns.[7]

The surface states and the electronic structure of the $c(4\times2)$ surface are similar to those of the $p(2\times1)$. Close to the top of the valence band are two groups of four surface states with π character; these come from the small splitting of the bonding and antibonding states with π character, which takes place when the symmetry is lowered from $p(2\times1)$ to $c(4\times2)$ under tensile stress. Close to the CBB we find surface states with σ character: these are nonbonding states. A difference between the electronic structures of the $p(2\times1)$ and $c(4\times2)$ reconstructions can be seen in the electronic density of states: below the Fermi level (E_F), the shoulder originating from surface states is more pronounced for the $c(4\times2)$ than for the $p(2\times1)$ reconstruction. This difference between the valence-band spectra of $p(2\times1)$ and $c(4\times2)$ surfaces has been recently found experimentally.[23]

V. FINITE TEMPERATURE PROPERTIES OF Si-TERMINATED SURFACES

In Ref. 23 it is argued that both the ARUPS electronic spectra of the $c(4\times2)$ reconstruction, as well as the STM images of this surface, are modified when heating the system at $\simeq 700$ K, and show a transition to a metallic $p(2\times1)$ reconstruction. In order to make contact with these experiments we performed molecular-dynamics (MD) simulations of the $p(2\times1)$ reconstruction at 400 and 900 K. The main scope is to monitor changes in the geometry and in the electronic structure of the surface as the temperature is raised. These calculations were performed using 8 atoms per layer and 11 layers in the MD cell. A similar simulation for the $c(4\times2)$ reconstruction would imply the use of 176-atom MD cells (16 atoms per layer instead of 8), in order to have an equivalent k-point sampling on both surfaces in the supercell. Few picoseconds simulations with such a cell would correspond to a computational effort that is too big for the scope of the present, qualitative investigation.

When heating the $p(2\times1)$ reconstructed surface, we observed large fluctuations of the distance between dimers, which at 400 (900) K varies between $\simeq 2.4$ (2.2) and 3.0 Å, i.e., close to the value of the ideal structure (3.03 Å).[5] Therefore, during short time intervals, different disordered configurations are sampled, which do not retain the $p(2\times1)$ symmetry. This is a consequence of the flatness of the potential energy surface of the system, as atoms move in a plane parallel to the surface, which was observed when optimizing the surface geometry (see Sec. III A). We have computed the density of electronic states (EDOS) of 10 (15) geometrical configurations equally separated in time over our equilibration runs, and averaged the results to have the EDOS of the system at 400 (900) K. At 400 K the average gap is 0.25 eV, close to the value computed at 0 K (0.3 eV); at 900 K this value decreases to a rather small number, which is regarded as zero, within the accuracy of our calculation. However, the EDOS at the Fermi level is very small. Our results indicate that at $T \geqslant 400$ K the $p(2\times1)$ reconstruction of the Si-SiC(001) surface of an unstrained bulk is disordered; at least up to 400 K the surface is nonmetallic. A tendency to become metallic appears at temperatures well above 400 K. Given the elastic properties of Si-SiC(001) surfaces, it is conceivable to expect the $c(4\times2)$ reconstruction to be as well disordered at T of the order of 400 K, with no sharp transition to a higher symmetry reconstruction.

VI. STM IMAGES

A powerful way to analyze the electronic states of surfaces is provided by STM images. We have computed the tunneling current $I(x,y,z;V)$ and its derivative with respect to applied voltage V for both $p(2\times1)$ and $c(4\times2)$ surfaces. The calculations have been carried out using the Tersoff-Hamman approximation,[24] with $\partial I(x,y,z_0;V)/\partial V \propto \Sigma_i |\psi_i(x,y,z_0)|^2 f'(\epsilon_i + eV)$. Here, $\psi_i(x,y,z)$ are Bloch functions and ϵ_i their corresponding eigenvalues, f' is the derivative of the Fermi distribution, and z_0 is the distance from the surface at which the calculation is performed.

A. Clean surfaces

We first considered neutral clean surfaces and computed $\partial I(x,y,z_0;V)/\partial V$ and constant current profiles for $V=-1.5$ eV. These are reported in Fig. 1 for both $p(2\times1)$ and $c(4\times2)$ reconstructed surfaces: $\partial I(x,y,z_0;V)/\partial V$ images (top panel) show the π-like bonding states on the dimers. Bright spots appear on all dimers of the $p(2\times1)$ dimer rows (left); on the contrary, only the up dimers are visible on the $c(4\times2)$ rows (right). Constant current plots show surface states having large components *between* dimers. These are bonding and antibonding π-like states. Depending on their position in the surface Brillouin zone, both bonding and antibonding π-like Bloch states can have lobes tilted away from the dimers, overlapping with those of adjacent rows, since the distance between dimers is relatively small. States with maxima localized between dimers give rise to bright spots of $I(x,y,z;V)$ between dimers. On the $p(2\times1)$ surface these spots are identical on all dimers, while on the $c(4\times2)$ surface they clearly show the difference in height between up

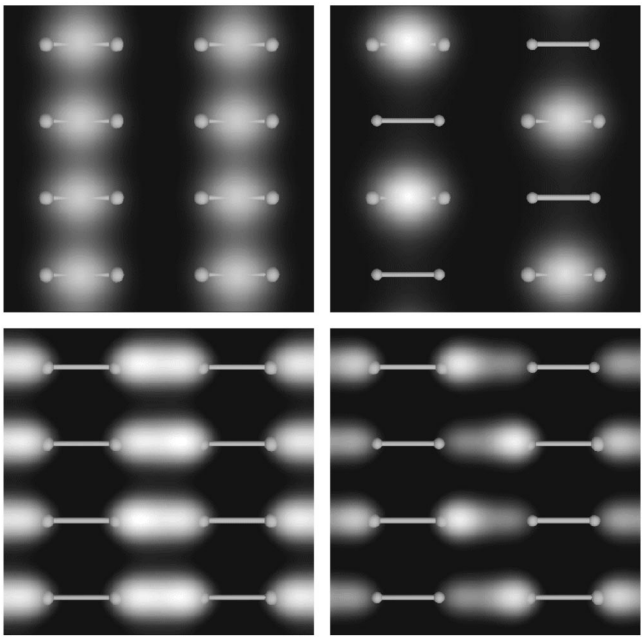

FIG. 1. Computed STM images of the $p(2\times1)$ (left panel) and $c(4\times2)$ (right panel) reconstructions of Si-SiC (001): the upper and lower panels show a plot of $\partial I(x,y,z_0;V)/\partial V \propto \Sigma_i |\psi_i(x,y,z_0)|^2 f'(\epsilon_i+eV)$ (see text) and of a constant current profile, respectively; in both cases $V=-1.5$ eV. Here $I(x,y,z;V)$ is the tunneling current computed within the Tersoff-Hamman approximation (Ref. 24) at a given applied voltage V; the constant current profile shows all z values between the surface and the top of the slab, such that I equals a given value I_0.

and down dimers. This difference (Δz), as estimated from experimental STM images,[8] is 0.1 Å, which is larger than the value obtained in our work for the case directly comparable with experiment. Since the model used in Ref. 8 to estimate Δz is different from ours and in our calculations we did not include the effect of the tip electric field on the sample, a quantitative comparison between experiment and our work is not straightforward.

STM images at positive voltage (not displayed) do not show appreciable differences between the $p(2\times1)$ and $c(4\times2)$ surfaces, the largest contribution coming from σ surface states in both cases. We note that experimentally the empty surface states might not be visible due to large tip-induced band bending,[25] and to the negative electron affinity of the surface.

In order to investigate how the calculated images depend on voltage, we repeated the calculation of a constant current image for the $c(4\times2)$ reconstruction at $V=-3$ eV. This is displayed in Fig. 2. At variance with the corresponding image at $V=-1.5$ eV (right-bottom panel of Fig. 1), we find spots localized also on dimers, showing the difference in height between up and down dimers. As expected, lowering the voltage makes the bonding π states have a larger contribution to the tunneling current. The image at $V=-3$ eV is in satisfactory agreement with measured[8,9] images at constant current, at the same voltage. However, the measured images show larger components on dimers and thus resemble very closely the computed images in the $\partial I/\partial V$ mode. This means that in our calculation of $I(x,y,z;V)$, antibonding components of surface states are weighted more than experimentally. This difference between theory and experiment may be related to the tip induced electric field, which could change the energy separation between π and π^* surface states. Such a field was not included in our study. The influence of a constant electric field on the surface structure has been studied recently for Si(001), using *ab initio* calculations.[26] The authors have shown that for a field directed towards the surface (as in a STM experiment, for which the electrons tunnel out of the surface), the electronic charge is pulled out from the surface towards the vacuum. The presence of this polarization charge affects the surface geometry, in particular the relative position of upper and lower dimer atoms, the upper one moving towards the vacuum and the lower one towards the slab by an amount of about 0.16 Å. Consequently, the dimer bond length and buckling angle are changed. Given the flatness of the potential energy surface of Si-SiC(001) in the plane of the surface, it is reasonable to expect the tip induced electric field to modify the dimer bond lengths and thus the relative position in energy of π, π^*, and σ states. In particular, if a polarization charge accumulates at the surface, the Si-C bonds between the first and second surface layer will be weakened and could become longer, thus allowing shorter surface dimers to form. These would give rise to STM images, where the weight of bonding π states is larger than in the absence of an induced field.

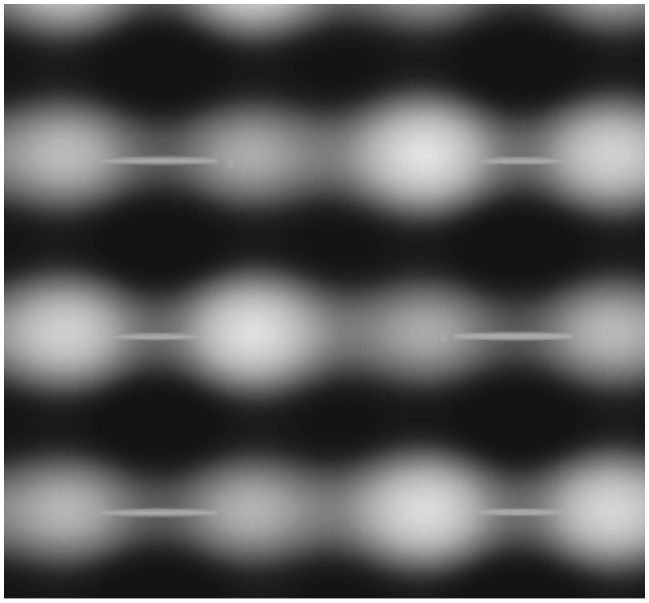

FIG. 2. Constant current profile for the $c(4\times2)$ reconstruction, for $V=-3$ eV. This has to be compared with the corresponding plot for $V=-1.5$ eV, displayed in the bottom right panel of Fig. 1.

Another difference between computed and measured STM images could come from the property of the surface to lose electrons, due to its negative electron affinity. Therefore, we have computed STM images of a positively charged surface. These have to be considered in a qualitative manner, since in our calculation the missing charge per atom is very large ($\simeq 0.4$ electrons per surface atom). When the surface is charged positively and the dimers have a stronger bond than in the neutral case, both constant current and dI/dV images show bright spots on the dimers, to indicate the large weight of bonding surface states. The images obtained in the two different modes closely resemble each other, similar to ex-

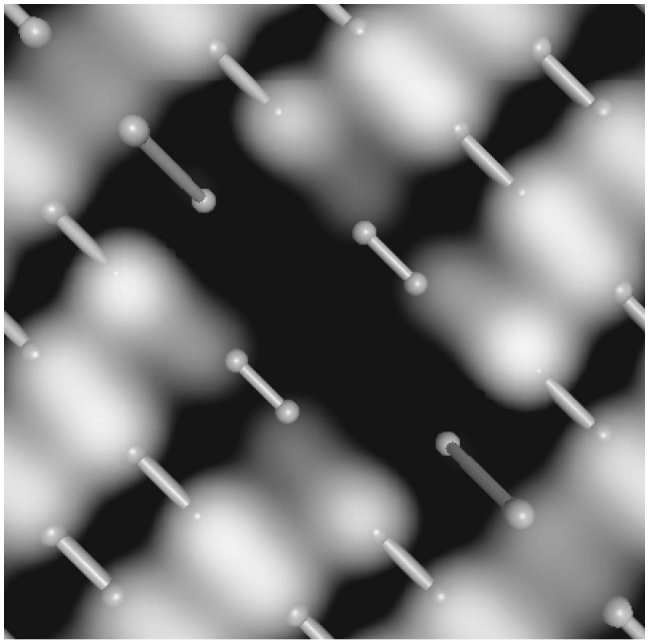

FIG. 3. Constant current profile (Ref. 24) of the unstrained $p(2\times1)$ surface with a missing dimer, at $V=-1$ eV. The bond length of the two dimers parallel to the defect is 2.37 Å and that of the two adjacent buckled dimers in parallel rows is 2.46 Å.

periment. On the contrary, when the surface is negatively charged and the bonds between dimers are weakened, bright spots appear *between* dimers in constant current images, similar to the neutral case.

B. Missing dimer

Figure 3 shows a calculated constant current image of the $p(2\times1)$ surface with a missing dimer, for $V=-1.0$ eV. The bright spots are located between adjacent dimers. The short dimers around the defect are not visible since their z coordinate is much lower (0.15 Å) than that of the other atoms. This gives rise to a dark area much bigger than the size of the missing dimer. This image can help to interpret STM data,[9] where $c(4\times2)$ and $p(2\times2)$ domains have been seen to coexist, and where the transition between domains apparently occurs in regions of missing dimers.

VII. CONCLUSIONS

In summary, we have studied several physical properties of Si-terminated SiC(001) surfaces, including the influence of stress and defects on the surface reconstruction, and the effect of temperature and extra charges on the geometrical and electronic properties of the system. The reconstruction of Si-SiC(001) does not involve either important hybridizations or the formation of strong bonds, at variance with what is observed on the corresponding surfaces of Si and C. Moreover, the potential energy of the system is extremely flat as surface atoms move in the plane parallel to the surface, which gives rise to unique elastic and electronic properties.

In our calculations we have found that an unstrained bulk exhibits a $p(2\times1)$ reconstruction, which is under tensile stress. We have shown that missing dimers allow the surface to relieve stress and help stabilize the $p(2\times1)$ reconstruction. The $p(2\times1)$ reconstructed surface is nonmetallic at least up to 400 K, and already at this temperature it becomes considerably disordered. Small applied stresses were found to lower the symmetry of the surface reconstruction from $p(2\times1)$ to $c(4\times2)$. This suggests that residual stresses in SiC grown on Si are responsible for the different reconstruction patterns observed experimentally. The $c(4\times2)$ pattern obtained in our simulations is in excellent agreement with recent experimental results. In particular, an accurate comparison between computed and measured STM images has permitted an interpretation of the experimental data. Finally, our results indicate that perturbations of the surface leading to a charging of the system may substantially affect its geometry: in particular, when the system is positively charged, we observe stronger bonds between dimers and shorter dimer bond lengths. This result is particularly relevant, due to the calculated negative electron affinity of the Si-SiC(001) surface.

ACKNOWLEDGMENTS

We are indebted to V. Bermudez for many useful comments and suggestions. We would like to thank A. Baratoff, N. Holzwarth, and A. Rizzi for useful discussions. This work was supported by the Swiss NSF and the Italian CNR (A.C.) through a FNS-CNR cooperation.

[1] V. Bermudez, Phys. Status Solidi B **202**, 447 (1997); J. Pollman, P. Krüger, and M. Sabisch, *ibid.* **202**, 421 (1997).
[2] See, e.g., MRS Bull. **22** (1997).
[3] J. Long, V. Bermudez, and D. Ramaker, Phys. Rev. Lett. **76**, 991 (1996).
[4] M. Sabisch *et al.*, Phys. Rev. B **53**, 13 121 (1996).
[5] A. Catellani, G. Galli, and F. Gygi, Phys. Rev. Lett. **77**, 5090 (1996).
[6] J. Powers, A. Wander, M. vanHove, and G. Somorjai, Surf. Sci. Lett. **260**, L7 (1992).
[7] M. Shek, Surf. Sci. **349**, 317 (1996).
[8] P. Soukiassian *et al.*, Phys. Rev. Lett. **78**, 907 (1997).
[9] J. Kitamura *et al.* (unpublished).
[10] P. Käckell, F. Bechstedt, H. Hüsken, B. Schröter, and W. Richter, Surf. Sci. **391**, L1183 (1997).
[11] V. Bermudez and J. Long, Appl. Phys. Lett. **66**, 475 (1995).
[12] For a review see, e.g., D. Vanderbilt in *Quantum Theory of Real Materials*, edited by J. R. Chelikowsky and S. G. Louie (Kluwer Academic, 1996), p. 251.
[13] For a review see, e.g., G. Galli and A. Pasquarello, in *Computer Simulation in Chemical Physics*, edited by M. P. Allen and D. J. Tildesley (Kluwer, Dordrecht, 1993), p. 261; M. C. Payne, M. P. Teter, D. C. Allan, T. A. Arias, and J. D. Joannopoulos, Rev. Mod. Phys. **64**, 1045 (1993).
[14] We used the first principles molecular dynamics programs BASIC96 and JEEP (http://irrmawww.epfl.ch/fg/jeep/jeep.html).

[15] D. Hamann, Phys. Rev. B **40**, 2980 (1989).
[16] V. Fiorentini and M. Methfessel, J. Phys.: Condens. Matter **8**, 6525 (1996).
[17] A. Ramstad, G. Brocks, and P. Kelly, Phys. Rev. B **51**, 14 504 (1995).
[18] J. Furthmueller and G. Kresse, Phys. Rev. B **53**, 7334 (1996); P. Krüger and J. Pollmann, Phys. Rev. Lett. **74**, 1155 (1995).
[19] Calculations at $E_{\mathrm{cut}}=40$ (58) Ry with 11 and 19 layers and 8 atoms per layer give $\gamma=1.71(1.99)$ and 1.84 eV/atom, respectively. When using 11 layers and 16 atoms per layer we obtain 1.54 eV/atom. We therefore estimate an error of ± 0.25 eV/atom on γ.
[20] A. Garcia and J. Northrup, Phys. Rev. B **48**, 17 350 (1993).
[21] H. Ibach and J. E. Rowe, Phys. Rev. B **10**, 710 (1974).
[22] A. Baldereschi, S. Baroni, and R. Resta, Phys. Rev. Lett. **61**, 734 (1989).
[23] V. Yu. Aristov *et al.*, Phys. Rev. Lett. **79**, 3700 (1997).
[24] J. Tersoff and D. Hamann, Phys. Rev. B **31**, 805 (1985).
[25] M. McEllistrem, G. Haase, D. Chen, and R. Hamers, Phys. Rev. Lett. **70**, 2471 (1993).
[26] H. Ness and A. J. Fisher, Phys. Rev. B **55**, 10 081 (1997).